

DOI 10.14622/Advances\_48\_2022\_11

## Comparison of the performance of DLC to chromium as wear resistance layer on a gravure cylinder for printing fine line structures

Laura Cirstea, Anna Kolesova, Hammad Khan, Mohamed Abouelmagd, Swapnil Patel, Thomas Sprinzing, Matthias Galus and Armin Weichmann

Hochschule der Medien Stuttgart, Institut für Angewandte Forschung (IAF), Nobelstr. 10, 70569 Stuttgart, Germany

E-mails: lc035@hdm-stuttgart.de; ak280@hdm-stuttgart.de; hk060@hdm-stuttgart.de; ma120@hdm-stuttgart.de;

p099@hdm-stuttgart.de; sprinzing@hdm-stuttgart.de; galus@hdm-stuttgart.de; weichmann@hdm-stuttgart.de

### Short abstract

For many decades in rotogravure electro plating a chromium layer on top of the copper surface which holds the cells was used as wear protection for the print form cylinder. Recently, coating the copper with a layer of diamond like carbon (DLC) presents an alternative with even higher wear protection. The price of a DLC coating is significantly higher, so further advantages would be beneficial to justify its application. There were indications that the ink accepting and releasing properties of the DLC are superior to chromium. This would be especially useful for micro structures and fine lines. Therefore, we designed a print form including many different small structures and manufactured two identical cylinders by laser mask etching, one electro plated with chromium, one coated with DLC. A print trial was conducted on our industrial-scale gravure printing machine. We compared the two surfaces with black ink on a white biaxially oriented polypropylene (BoPP) film under varying ink viscosities, doctor blade materials and doctor blade angles. Analysis of print gradation, missing dots and mottle was made, a visual assessment of a fine line star pattern was conducted and 15  $\mu\text{m}$ , 20  $\mu\text{m}$ , and 50  $\mu\text{m}$  lines in and across the print direction were measured according to their average width and homogeneity. Almost every evaluation shows the micro structures printed were significantly better with the DLC surface. The influence of the surface surpassed by far the other parameters. The ink viscosity had surprisingly low influence. This indicates that the difference of the surfaces in respect to print quality indeed is based on their different ink releasing capabilities, constituting DLC superior to chromium.

**Keywords:** rotogravure, diamond like carbon, micro structures, quality control

## 1. Introduction and background

One of the challenges that the global gravure printing industry is facing is its homologation in line with the requirements of sustainable printing. Finding environmentally friendly alternatives to electro plating of the rotogravure cylinders with Chromium(IV) is an urgent matter of research, mainly due to the environmental hazard of this element in its ionic state. The Green Gravure project aims exactly at this, and one solution developed by the Roto-Hybrid Group is coating of the copper with a layer of Diamond like Carbon (DLC). The Roto Hybrid Process<sup>®</sup> was already part of various pilot studies in Europe and USA, at Mondi Group and Western Michigan University. This new technology presented even better properties in wear protection of the cylinder, print quality and surface smoothness. Moreover, among the advantages are a reduction in ink usage of up to 10 %, an increase in the cylinders' lifetime of 500 %, a decrease in storage space for the print jobs of 80 %, a reduction in time of cylinder readiness to print of 50 %, and the elimination of the chromium oxide layer. Due to its high production cost, the sector that would benefit the most from the change to DLC coating is security printing (European Commission, 2022). In fact, the reproduction quality

of micro structures and fine lines, along with wear protection, is the main aspect that interests this sector. This paper investigates if DLC can satisfy or even exceed these requirements compared with chromium.

## 2. Materials and methods

Fluid transfer in gravure printing is a complex process. In the last decades, researchers like Kunz (1975), Hübner (1991), Kumar (2015), Grau, et al. (2016) and Schäfer, et al. (2019) have contributed to a deeper understanding. More recently, Brumm, et. al. (2021a; 2021b) tried to classify transfer patterns on the basis of a neural network. This paper uses a design of experiments (DoE) to compare the performance of the DLC surface versus the standard hard plated chromium surface with a specific focus on very fine structures.

### 2.1 Printing form layout

The company GRT (GRT GmbH, Hamm, Germany) used two identical gravure cylinders with a basic copper roughness of  $r_z = 0.37 \mu\text{m}$  ( $r_z$  is defined as the average of the difference between the tallest “peak” and the deepest “valley” in the surface within 5 traces of 0.25 mm length) to produce the print form with the Think Laser process (Think Laboratory, Kashiwa, Japan). This process utilises a laser generated mask with a laser spot size of  $2 \mu\text{m}$  to etch the micro structures into the copper. The etching depth was  $9 \mu\text{m}$ . The print form was designed to contain various small structures and patterns in a total format of  $700 \text{ mm} \times 590 \text{ mm}$  (Figure 1). The chrome plating (layer thickness  $5\text{--}7 \mu\text{m}$ ) was also performed by GRT, and the DLC coating (layer thickness  $5\text{--}7 \mu\text{m}$ ) was performed by RotoHybrid (Roto-Hybrid Gravure Technologies, Wuppertal, Germany).

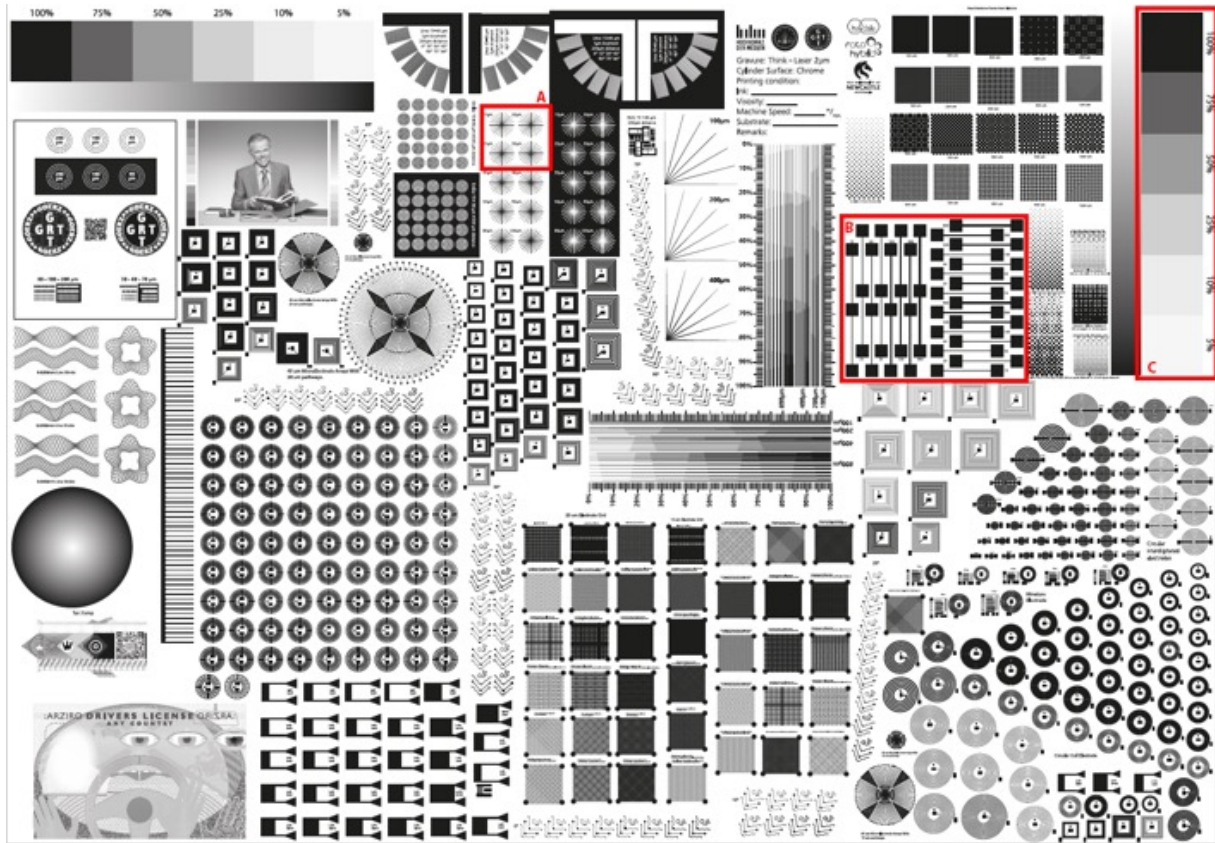


Figure 1: Upper half of printing form layout ( $350 \text{ mm} \times 590 \text{ mm}$ ); the complete form ( $700 \text{ mm} \times 590 \text{ mm}$ ) consists of the upper part and the lower part, the lower part uses a  $180^\circ$  rotation of the upper part

## 2.2 Gravure printing trial

The print trial was conducted on an industrial-scale gravure printing machine, with black ink on white biaxially oriented polypropylene (BoPP) film. The following print conditions apply for the trial:

- *Gravure press*: BOBST ROTOMECH MW 60, press speed: 150 m/min, cylinder circumference: 700 mm, cylinder bale width: 700 mm, pressure roller hardness: 75 shore A, pressure roller pressure: 1.5 bar, doctor blade pressure: 1.5 bar, dryer temperature: 60 °C with 10 % recirculation, corona treatment: 20 W·min/m<sup>2</sup>. No electrostatic assist (ESA) was used during the DoE, except for one additional trial point.
- *Substrate*: WSS 20 BoPP solid white film, both sides heat sealable, treated (Taghleef Industries, Dubai, United Arab Emirates)
- *Ink*: Siegwirk series NC 133-4, black (Siegwerk Druckfarben, Siegburg, Germany) used together with extender NC 133-15 Extender Varnish G0 (Siegwerk Druckfarben, Siegburg, Germany) in a blend of two parts basic ink, one part extender.
- To dilute to print ready ink a solvent mixture of ethyl acetate CAS 141-78-6 (70 %) and ethanol CAS 64-17-5 (30 %) was used.
- *Doctor blades*: Two different doctor blades were used – Swedcut MicroKote G, 40 mm × 0,15 mm Standard Lamella (Swedev AB, Munkfors, Sweden) and MDC 40 mm × 0.150/0.065 mm × 1.3 mm, type No. 01040001500.02534, Roll #16 1 003110.01 (Daetwyler SwissTec, Bleienbach, Switzerland).

## 2.3 Design of experiments

The print trial was started by determining a good print quality with good adhesion to the BoPP substrate. This was used as the reference quality and determined the medium setting of the DoE: doctor blade Swedcut MicroKote G, doctor blade angle 55°, ink viscosity 19.8 s/ISO#4, cylinder type chromium.

The following DoE variables resulted in a total count of 36 trial points:

- *Cylinder surfaces*: chromium (Cro), diamond like carbon (DLC)
- *Ink viscosities*: 17.1 s, 19.8 s, 23.1 s measured with a 4 mm ISO flow cup (DIN EN ISO 2431, No. 322 Erichsen, Hemer, Germany)
- *Doctor blade types*: Swedcut MicroKote G, MDC Type No. 01040001500.02534
- *Doctor blade angles*: 48°, 55°, 60°

## 2.4 Sample analysis

The target functions of the DoE were print gradation, mottle of the solid, number of missing dots per area, line homogeneity and line width of fine lines, and quality assessment of a fine line star pattern.

### 2.4.1 Gradation measurements

Density measurements were performed on the tonal values (100 %, 75 %, 50 %, 25 %, 10 %, 5 %; screen frequency 100 lines/cm) in part C of the printing form layout with a Techkon SpectroDens Spectro-Densitometer (TECHKON GmbH, Germany).

### 2.4.2 Mottle index measurements

Mottle index measurements were performed on the 100 % tonal value field in part C. The overall mottle index is determined within a 300 dpi grid calculated by downscaling the 1200 dpi image. The evaluation program is written in Java by Weichmann (2015) based on the algorithm by Rosenberger (2002).

It works on an area of 256 × 256 pixels, resp. 21.67 × 21.67 mm. It segments this area into squares that subsequently increase in size over 7 steps: 85 µm, 170 µm, 340 µm, 680 µm, 1.34 mm, 2.68 mm, 5.42 mm

edge length. For each size it calculates the mean of the absolute differences of the means of the grey values of the four sub-squares contained in each of these squares. Then it takes the mean of these means, multiplied by the standard deviation of these means, and multiplied by the standard deviation of the mean of the grey values of the squares. This results in a value for each size of squares. Finally, the mottle index is the mean over these 7 values.

The greater the value of the mottle index the more mottle is detected. An overall mottle index greater than 10 indicates well visible structures. Lower numbers but above 1 are associated with less severe mottle, however visible. Values below 1 indicate a nice homogeneous ink surface.

#### 2.4.3 Missing dots analysis

In part C the tonal values of 50 %, 25 % and 10 % in a screen frequency of 100 lines/cm were used to count the missing dots per area. The evaluation program is written in Java by A. Weichmann (2015) and works with 1 200 dpi images. It utilizes edge filtering and adaptive dot size filtering to reliably count the number of missing dots in these fields and normalise them to  $\text{cm}^2$ . As missing dots distort the image and decrease the image quality, fewer missing dots are better.

#### 2.4.4 Fine line analysis

In part B fine lines with a nominal width of 15  $\mu\text{m}$ , 20  $\mu\text{m}$  and 50  $\mu\text{m}$  in-web and in cross-web direction were measured according to their width and homogeneity and additionally evaluated for their difference in the two directions. The evaluation program “Line Analysis for Printed Lines” is written in Java by A. Weichmann (2021). It utilizes an USB microscope (TOOLCRAFT USB Microscope,  $2\,592 \times 1\,944$  pixels, magnification factor 200), with which a single line is captured. For analysis, the line is rotated into a horizontal position, then in every pixel column the upper and lower border is determined by a threshold operation (66 % of the brightness between darkest pixel and substrate white). After calculating the regression line of all pixels of a border, to exclude dents in the border or small holes within the line, 30 % of the pixels which have the greatest distance to the regression line are eliminated. With the residual 70 % the final regression line is calculated and determines this border of the line (Figure 2). The distance between the regression lines of the upper and the lower border defines the measured line width.

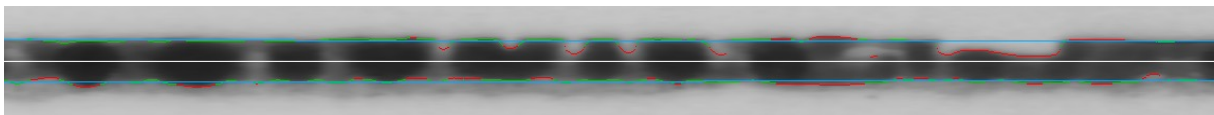


Figure 2: Fine line with nominal width 20  $\mu\text{m}$  analysed in “Line Analysis for Printed Lines”; blue pixels: regression lines for borders, green pixels: border pixels for final regression (70 %), red pixels: 30 % of border pixels too far from regression line and therefore not used for final regression, white line: centre line between the two border lines

From the pixels of the middle area of the line ( $\pm 2$  pixels around the centre line between the two border lines) the standard deviation is calculated. This number serves as the measure for homogeneity, i.e. the higher its value the less homogenous the reproduction of the line.

Figure 3 shows all lines measured for chromium and DLC for the trial point with viscosity 19.8 s #4, doctor blade Swedcut, angle 55°. Every line of chromium alternates with its counterpart of DLC surface. As expected, the cross-web lines reproduce much better than the in-web lines. Clearly the DLC lines are more defined. Especially the in-web direction lines are much better reproduced. The chromium 15  $\mu\text{m}$  (3) line is not reproduced at all and the 20  $\mu\text{m}$  line (7) is printed as fragments only, while the DLC lines are not perfect but recognizable as lines. The line DLC 50  $\mu\text{m}$  cross-web (10) is overly wide, as the high ink volume with this line depth leads to smearing.

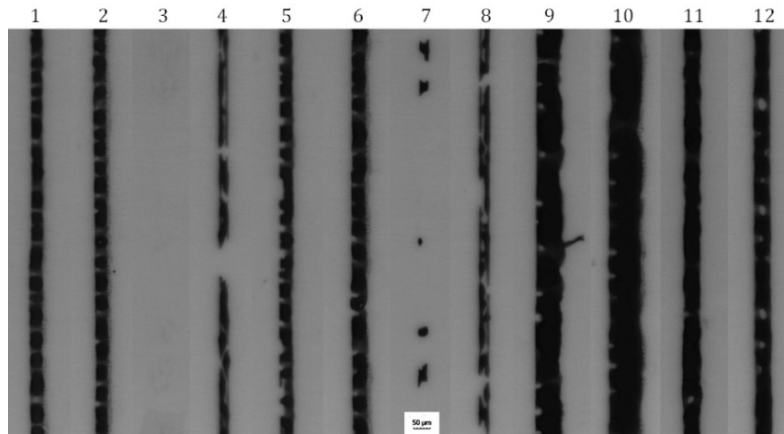


Figure 3: Example of lines, trial point with viscosity 20 s #4, doctor blade Swedcut, angle 55°, no ESA; 1: Cro 15 µm cross-web, 2: DLC 15 µm cross-web, 3: Cro 15 µm in-web (no line at all), 4: DLC 15 µm in-web, 5: Cro 20 µm cross-web, 6: DLC 20 µm cross-web, 7: Cro 20 µm in-web, 8: DLC 15 µm in-web, 9: Cro 50 µm cross-web, 10: DLC 50 µm cross-web, 11: Cro 50 µm in-web, 12: DLC 50 µm in-web

#### 2.4.5 Visual assessment of fine line star pattern

The star pattern from area A of the print form (Figure 1) was cut out for every trial point and collected on one sheet to visually assess the quality of the fine line printing. The star pattern reproduces fine lines (15 µm, 20 µm, 25 µm, 30 µm) under many different angles and is especially sensitive to the homogeneity of the line and varying widths of the printed lines. The more homogeneous and uniform the widths of the lines under different angles, the better the quality. A scale was defined from 1 to 5 (Figure 4), where:

1. All lines are reproduced homogeneously
2. Some lines of 15 µm are fading away
3. Some lines of 15 µm are not printed and some lines of 20 µm are fading away
4. Some lines of 15 µm and 20 µm aren't printed, some lines of 30 µm are fading away
5. All lines have some disruptions and are not homogeneous

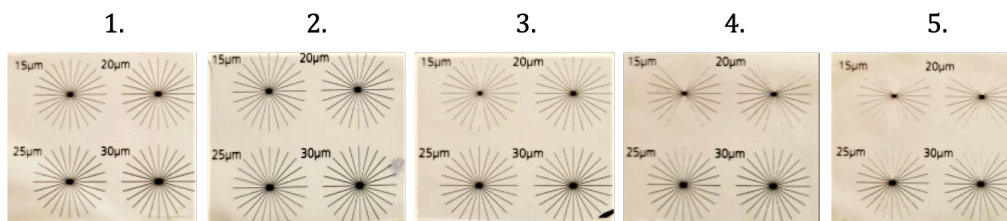


Figure 4: Examples of the five grades of star patterns with fine lines of 15 µm, 20 µm, 25 µm, and 30 µm from area A of the print form

The patterns were presented to 6 people, 3 with and 3 without printing background. Every person graded every trial point from 1 to 5 by looking at them with the help of a magnifying glass. The mean of all evaluators' gradings was used as a measure of the line quality.

### 3. Results and discussion

The density of the solids, the mottle, the missing dots and the fine line star patterns were analysed in MiniTab version 21.1.1 (Minitab, LLC, State College, Pennsylvania, USA). The Pareto diagram of the standardized effects and the main effects plot were used to graphically display the results.

### 3.1 Gradation measurements

The Pareto chart of the standardized effects for the solid density (Figure 5a) shows very clearly that the surface is by far the strongest factor of the DoE. Figure 5b shows that the DLC leads to a higher solid density than chromium. This is attributed to better cell emptying, and therefore more ink being transferred to the substrate. With DLC an average density of 2.26 was achieved, while chromium achieved only 1.91. The next relevant factor is the viscosity, where the best solid density was achieved with the lowest viscosity. The blade angle and its combination with the other factors, as well as the doctor blade on its own have a smaller influence, but they can still be considered significant. In fact, all the 4 factors, A, B, C, D, namely, surface, ink viscosity, doctor blade and blade angle, respectively, are over the significance threshold. The lower tonal values showed very similar results and are not detailed in this paper.

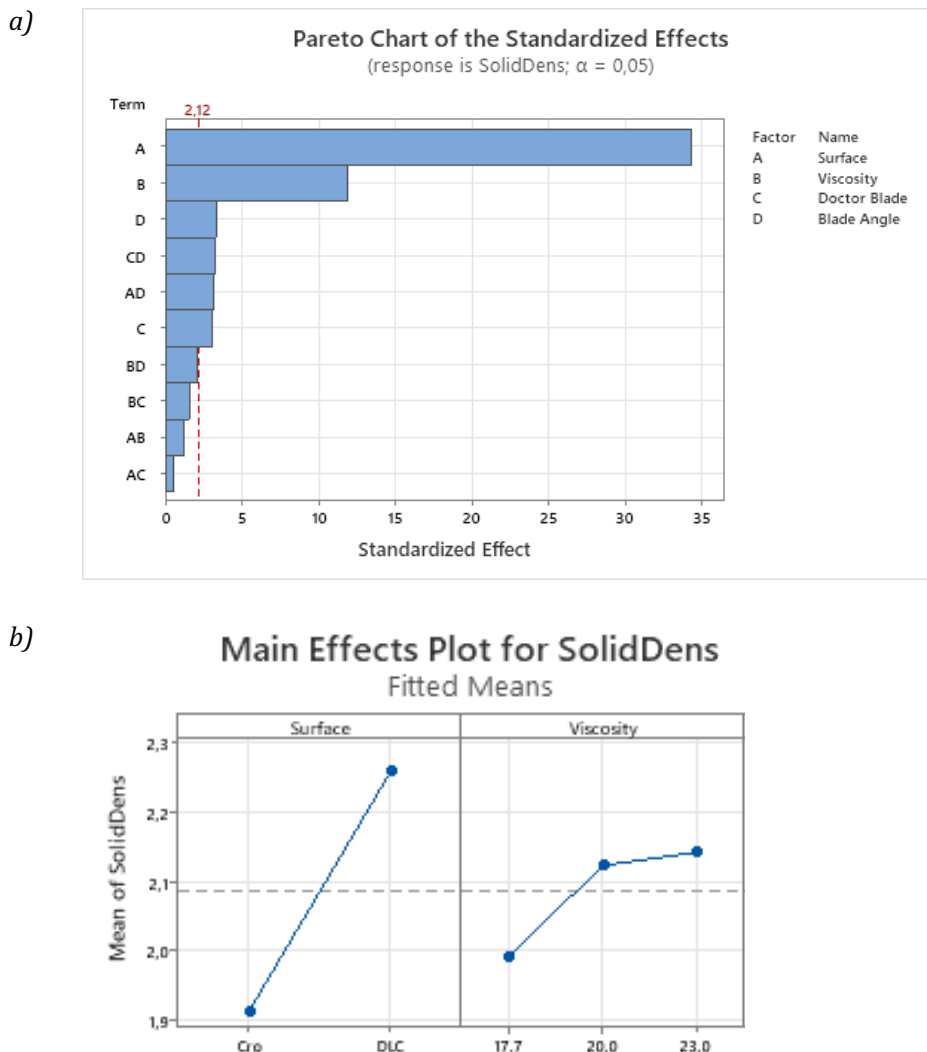


Figure 5: Pareto diagram of the standardized effects (a), and surface and viscosity plot (b) for the gradation measurements of the solid density, the red dotted line represents the significance level of 95 %

### 3.2 Mottle index measurements

The mottle index measurements show that the surface and its combination with ink viscosity are the most significant effects (Figure 6a). All the other parameters (viscosity, doctor blade and blade angle) and their combinations are quite far below the threshold. Indeed, the drying patterns depend on the amount of solvent in the ink. The best results were achieved with the highest viscosity and the chromium surface

(Figure 6b), the MDC doctor blade and the 55° blade angle. The DLC surface resulted worse for mottle, but this apparently negative result is caused by better cell emptying, that as mentioned above results in higher solid density, meaning that more ink volume was transferred. This increases the micro flow of the inks and the drying time and therefore these artefacts-related formations are facilitated. This effect, however, can be overcome easily by reducing the cell volume. In fact, 2.26 solid density is a high value (maximum was 2.44), and with smaller or more shallow cells a satisfying value of around 2.0 for the density can be achieved and consequently mottle reduced.

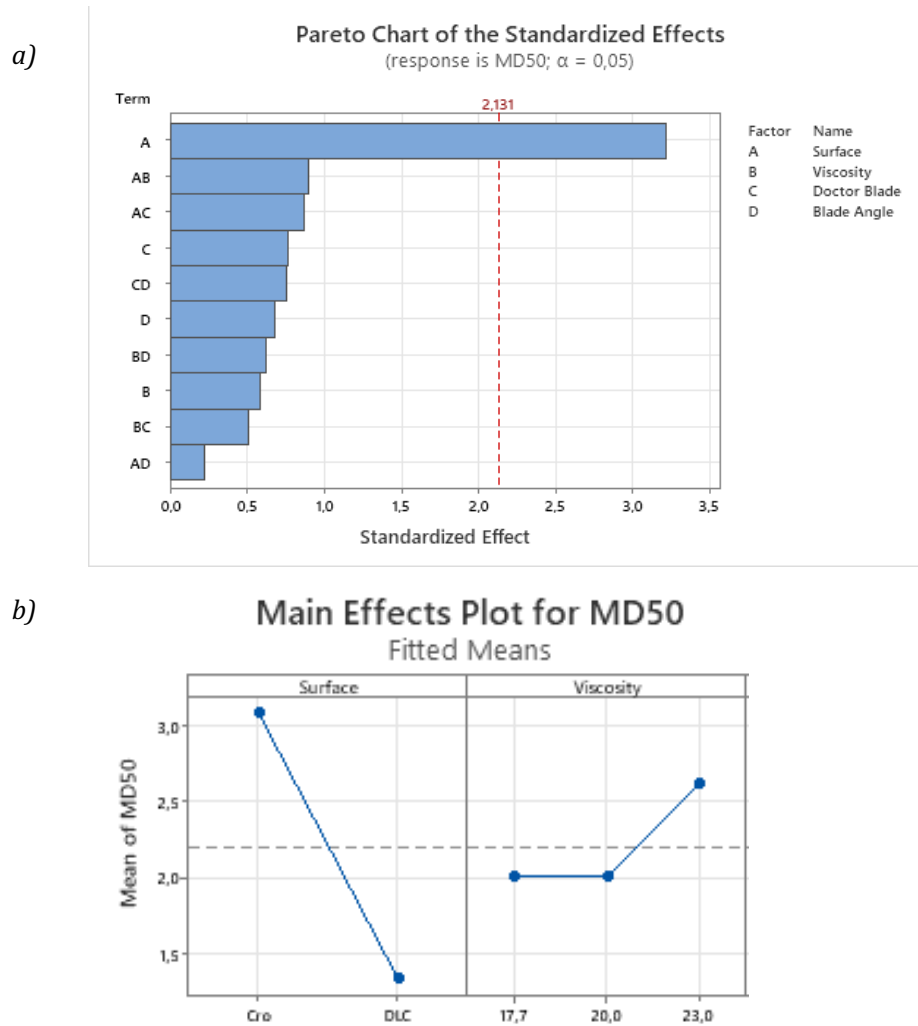


Figure 6: Pareto diagram of the standardized effects (a), and surface and viscosity plot (b) for mottle

### 3.3 Missing dots analysis

The average numbers of missing dots over all trial points normalised to  $\text{cm}^2$  are shown in Table 1. The number of missing dots is higher for a lower tonal value, i.e. the smaller the dots printed.

Table 1: Average number of missing dots over all trial points normalised to  $\text{cm}^2$

Coating	50 %	25 %	10 %
Chromium	3.1	200	1524
DLC	1.3	64	296

The missing dots per area at the tonal value of 50 % have a similar behaviour as at 10 %. In both cases the only significant parameter was the cylinder surface applied (Figure 7a). The other aspects could be neglected. The DLC surface performed clearly better, while the low and medium viscosity appeared to be favourable at the same level, for 50 % (Figure 7b), while for 10 % the best result was the opposite, i.e. with the highest viscosity the smallest dots could be reproduced better with less solvent, and, thus, more pigment and binder. For both 50 % and 10 % the Swedcut doctor blade and 48° blade angle provided the optimal choice.

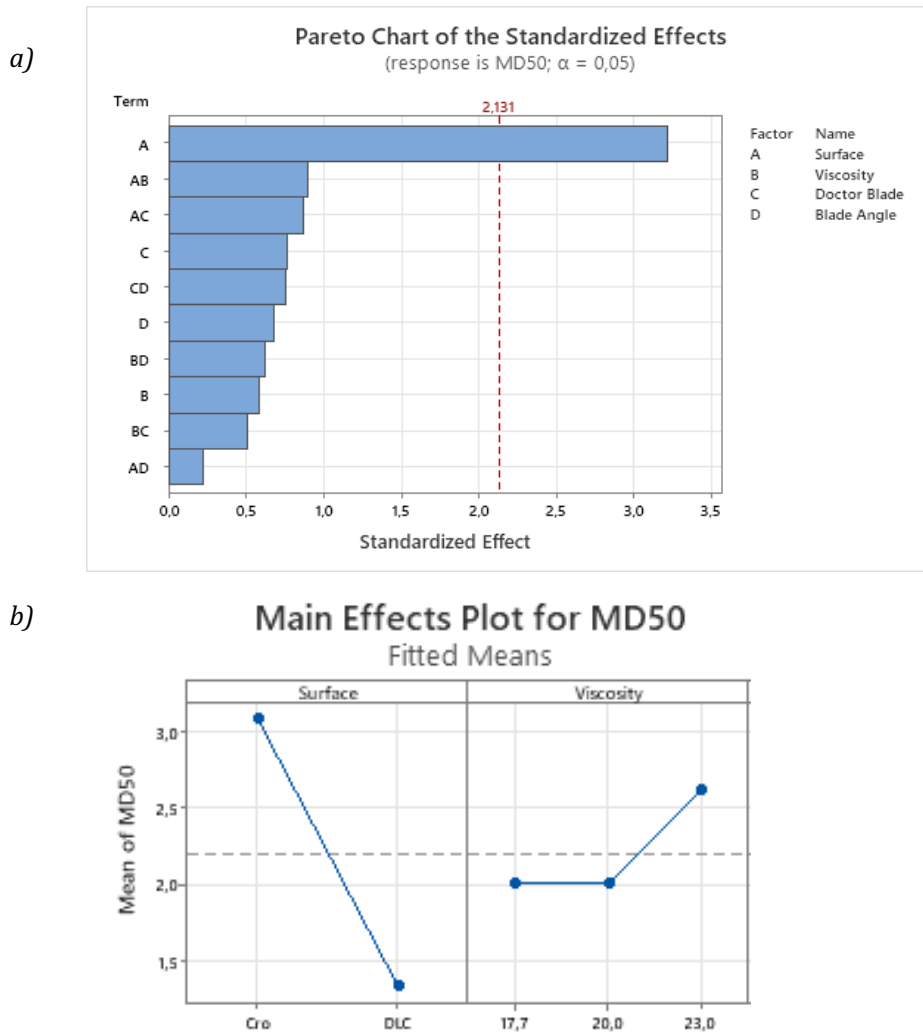


Figure 7: Pareto diagram of the standardized effects (a), and surface and viscosity plot (b) for missing dots in a patch of tonal value of 50 %

For the tonal value 25 % the most important parameter was the surface. In this case the viscosity was significant as well, though at a much lower level (Figure 8a). The missing dots per area at the tonal value of 25 % were counted least with the DLC surface and with the highest viscosity (Figure 7b). The Swedcut doctor blade had only slightly better values than the MDC, while the 48° blade angle was ideal.

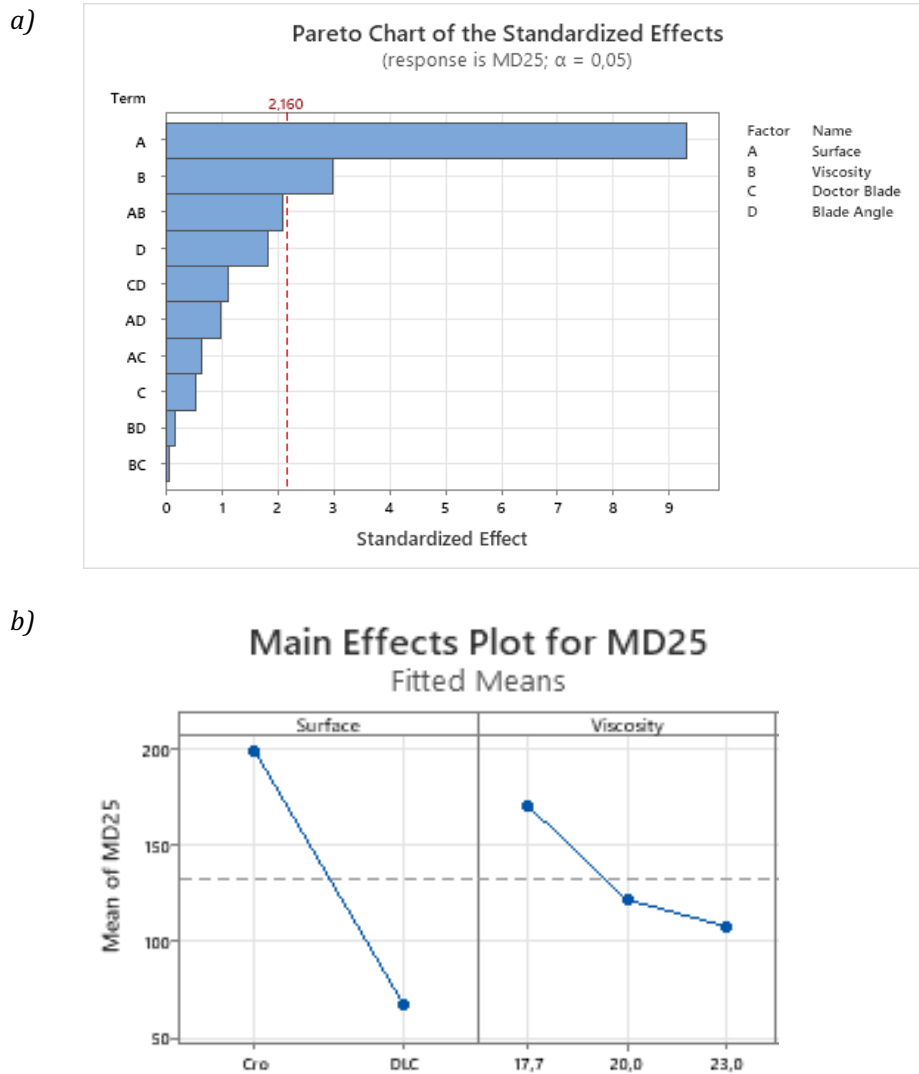


Figure 8: Pareto diagram of the standardized effects (a), and surface and viscosity plot (b) for missing dots in a patch of tonal value 25 %

### 3.4 Fine line analysis

Table 2 shows the average line width for 15  $\mu\text{m}$ , 20  $\mu\text{m}$  and 50  $\mu\text{m}$  lines in in-web and in cross-web direction. The line analysis was not possible at all for the in-web 15  $\mu\text{m}$  lines with chromium surface, as they did not print well enough to be analysed, in contrast to the DLC, where the lines were clearly defined. The lines appear reasonably spread with the DLC significantly wider than chromium. The cross-web lines are more than 10  $\mu\text{m}$  wider than the vertical ones, which is to be expected with the gravure printing process. As mentioned with Figure 3 the excessive spreading of the cross-web 50  $\mu\text{m}$  DLC line is due to smearing.

Table 2: Average line widths in  $\mu\text{m}$  over all trial points for chromium (Cro) and DLC for 15  $\mu\text{m}$ , 20  $\mu\text{m}$  and 50  $\mu\text{m}$  lines in in-web and in cross-web direction

Lines	Cro 15 $\mu\text{m}$	DLC 15 $\mu\text{m}$	Cro 20 $\mu\text{m}$	DLC 20 $\mu\text{m}$	Cro 50 $\mu\text{m}$	DLC 50 $\mu\text{m}$
cross-web	33.1	37.3	36.0	43.2	76.7	93.7
in-web	---	25.6	26.9	30.0	46.1	47.1

The homogeneity of the lines is also significantly better with DLC. As an example, the Pareto diagram and main effects plot of homogeneity of the cross-web 20  $\mu\text{m}$  line are shown in Figure 9.

Viscosity plays an important role as well. Surprisingly, higher viscosity results in better results. A 60° blade angle is preferred for cross-web line width and cross-web homogeneity. For in-web homogeneity the 48° is better. Swedcut is slightly preferred over MDC.

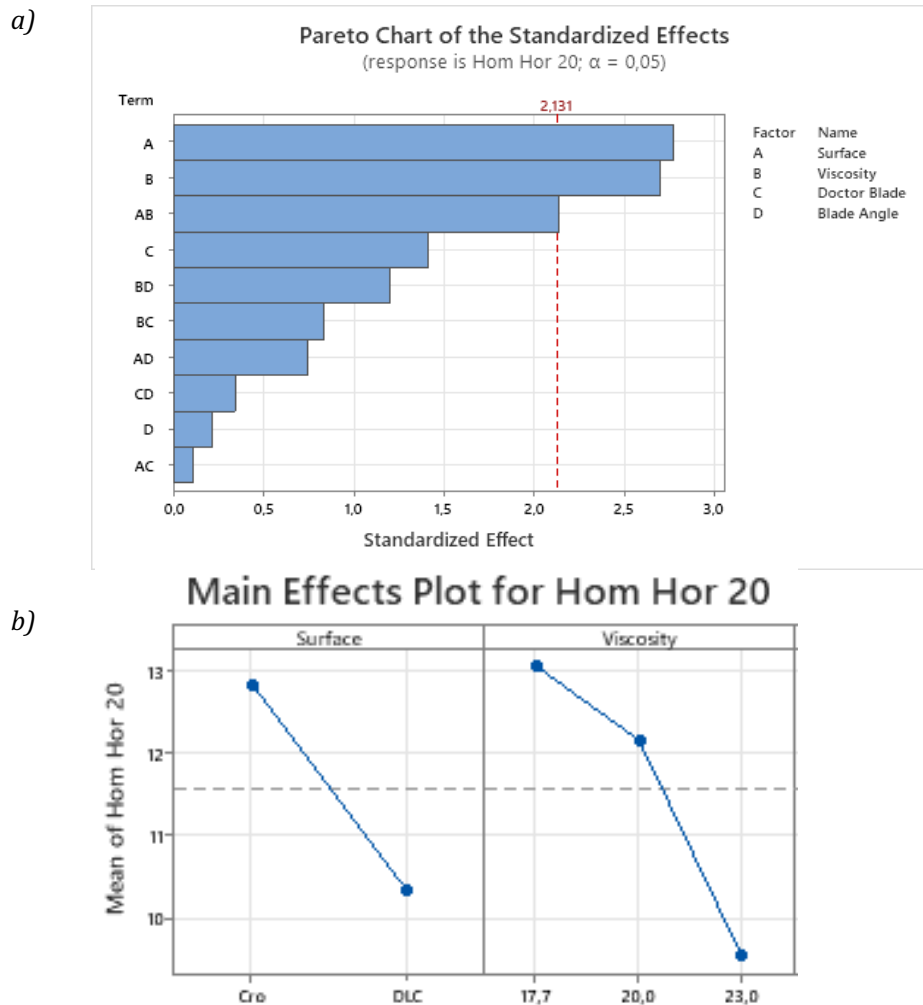


Figure 9: Pareto diagram of the standardized effects (a), and surface and viscosity plot (b) for homogeneity of the cross-web direction 20  $\mu\text{m}$  lines

### 3.5 Visual assessment of fine line star pattern

The Pareto analysis of the star pattern assessment shows a very clearly advantage of the DLC surface over the chromium surface. All other factors of the DoE are much weaker than this factor (Figure 10a). According to the results of the test, the DLC cylinder produces clearly more homogeneous printed lines (Figure 10b) with an average grade of 1.9. Samples which were printed with the Chromium cylinder showed much worse results (average 3.7). Especially the thin vertical lines could not be reproduced in most cases. After the cylinder's surface, the next factors that influence the print are in order of proportionality the viscosity, the blade angle, and their combination. The best results are achieved with medium viscosity and medium blade angle. The doctor blade plays a minor role.

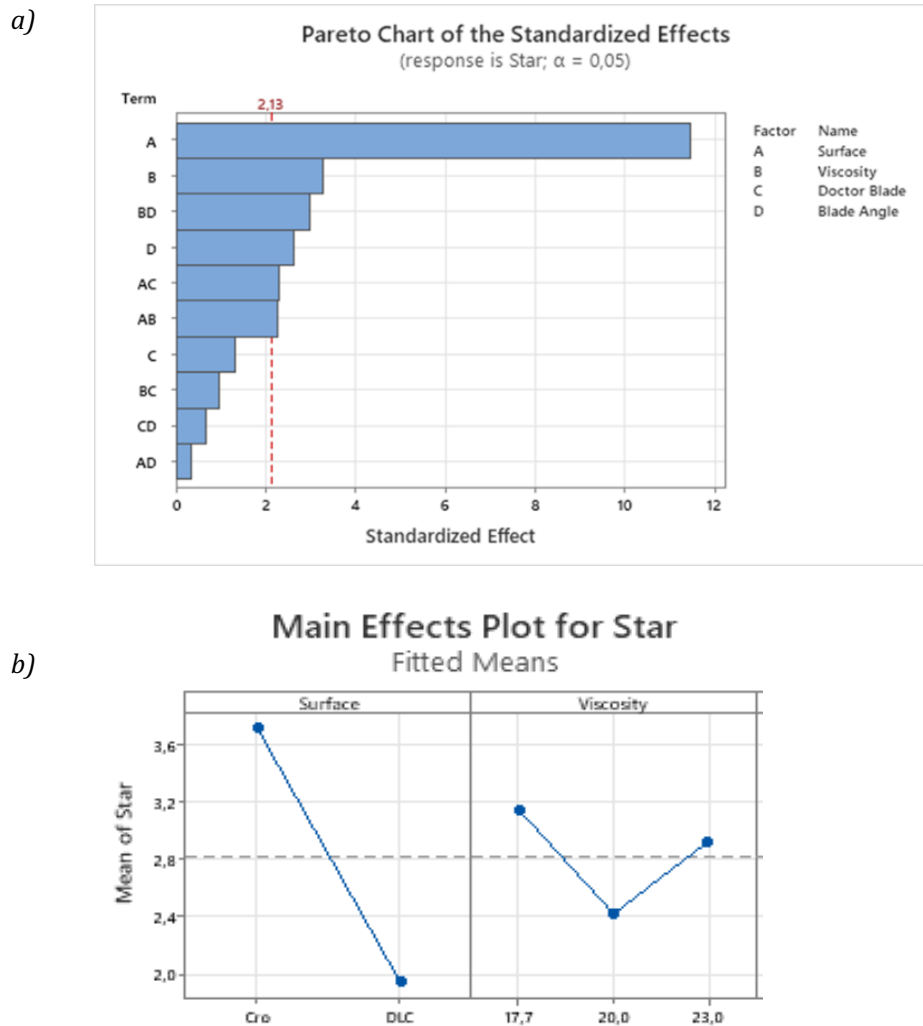


Figure 10: Pareto diagram of the standardized effects (a), and surface and viscosity plot (b) for the visual assessment of the star patterns

### 3.6 Surface energy

According to measurements by RotoHybrid the surface energy of the chromium plated cylinder's surface is in the range of 60 mN/m, while the surface energy of the DLC is in the range of 45 mN/m. Higher surface energies lead to a better wetting, i.e. filling of the cells. As organic solvents based gravure ink has typically a surface energy between 25 mN/m and 30 mN/m, which is significantly lower than these values, with both surface one can expect a good wetting. The ink release then is indeed an ink splitting. However, the point of splitting will lay the nearer to the surface the smaller the difference between the surface energies, therefore explaining at least part of the higher volume of ink transferred to the substrate with DLC.

Another factor is the thinner layer of DLC (4–5  $\mu\text{m}$  compared to 5–7  $\mu\text{m}$  for the chromium layer) which leads to a slightly larger cell volume of the DLC coated cells.

## 4. Conclusions and outlook

Practically each part of the print trial analysis has shown a crucial improvement in printing of micro structures and fine lines with DLC compared to traditional chromium plating. In every case of the DoE evalu-

ation the surface of the cylinder was the primary effect. In decreasing order, the viscosity, the blade type, and blade angle played a much smaller role in most cases. The smaller the structures the bigger the improvement. This indicates that the DLC surface has a significantly better ink releasing capability. This we postulate, as shown in the prior art, is due to a lower surface energy and a slightly thinner layer compared to the standard chromium surface. If microstructural properties of the surface play an additional role is to be shown in a future study.

Surely, this better performance together with the improved wear resistance is very interesting for high value applications like security printing and functional printing.

## Acknowledgements

We kindly thank GRT (GRT GmbH, Hamm, Germany) for manufacturing of the gravure cylinder forms and the chrome plating of one of them and RotoHybrid (Roto-Hybrid Gravure Technologies, Wuppertal, Germany) for DLC coating the other as well as sharing the surface energy measurements.

## References

- Brumm, P., Weber, T.E., Sauer, H.M. and Dörsam, E., 2021a. Ink splitting in gravure printing: localization of the transition from dots to fingers. *Journal of Print and Media Technology Research*, 10(2), pp. 81–93. <https://doi.org/10.14622/JPMTR-2016>.
- Brumm, P., Lindner, N., Weber, T. E., Sauer, H. M. and Dörsam, E., 2021b. A deep learning approach for the classification task of gravure printed patterns. In: C. Ridgway, ed. *Advances in Printing and Media Technology: Proceedings of the 47<sup>th</sup> International Research Conference of Iarigai*. Athens, Greece, 19–23 September 2021. Darmstadt: iarigai, pp. 2–9. [https://doi.org/10.14622/Advances\\_47\\_2021](https://doi.org/10.14622/Advances_47_2021).
- European Commission, 2022. *Periodic reporting for period 2 – green gravure (Roto-Hybrid Process® cylinders for green gravure printing)*. [online] Available at: <<https://cordis.europa.eu/project/id/738010/reporting>> [Accessed 25 March 2022].
- Grau, G., Cen, J., Kang, H., Kitsomboonloha, R., Scheideler, W.J. and Subramanian, V., 2016. Gravure-printed electronics: recent progress in tooling development, understanding of printing physics, and realization of printed devices. *Flexible and Printed Electronics*, 1(2): 023002. <https://doi.org/10.1088/2058-8585/1/2/023002>.
- Hübner, G., 1991. *Ein Beitrag zum Problem der Flüssigkeitsspaltung in der Drucktechnik*. Dr.-Ing. Dissertation. Technische Hochschule Darmstadt. <https://doi.org/10.25534/tuprints-00013550>.
- Kumar, S., 2015. Liquid transfer in printing processes: liquid bridges with moving contact lines. *Annual Review of Fluid Mechanics*, 47(1), pp. 67–94. <https://doi.org/10.1146/annurev-fluid-010814-014620>.
- Kunz, W., 1975. Ink transfer in gravure process. In: *TAGA Proceedings 1975: Annual meeting of the Technical Association of the Graphic Arts*. Toronto, Ontario, 1975. Rochester, NY, USA: TAGA, pp. 151–176.
- Rosenberger, R.R., 2002. *Mottle measurement of wet trap, back trap and other motley images*. [pdf] VERITY IA. Available at: <[https://www.verityia.com/\\_files/ugd/c4e5fa\\_efd8667d40f44c45a0187b99b2fb7559.pdf](https://www.verityia.com/_files/ugd/c4e5fa_efd8667d40f44c45a0187b99b2fb7559.pdf)> [Accessed 25 March 2022].
- Weichmann, A., 2015. *GravureQ: commercially available software for mottle and missing dots analysis*. Hochschule der Medien Stuttgart, Germany.
- Weichmann, A., 2015. *Line analysis for printed Lines*. Hochschule der Medien Stuttgart, Germany.